EUROPEAN ORGANIZATION FOR NUCLEAR RESEARCH

CERN-PPE/90-173

16 November 1990

Charged Particle Multiplicity Distributions in Z^0 Hadronic Decays

The DELPHI Collaboration

(Submitted to Zeitschrift für Physik C)

Abstract

This paper presents an analysis of the multiplicity distributions of charged particles produced in Z^0 hadronic decays in the DELPHI detector. It is based on a sample of 25364 events. The average multiplicity is $< n_{ch} > = 20.71 \pm 0.04(stat) \pm 0.77(syst)$ and the dispersion $D = 6.28 \pm 0.03(stat) \pm 0.43(syst)$. The data are compared with the results at lower energies and with the predictions of phenomenological models. The Lund Parton Shower model describes the data reasonably well. The multiplicity distributions show approximate KNO-scaling. They also show positive forward-backward correlations that are strongest in the central region of rapidity and for particles of opposite charge. These conclusions had already been obtained in the note CERN-PPE/90-117, which however was based on a data sample ten times smaller.

P.Abreu[16], W.Adam[37], F.Adami[28], T.Adye[27], G.D.Alexeev[12], P.Allen[36], S.Almehed[19], F.Alted[36], S.J.Alvsvaag[4], U.Amaldi[7], E.Anassontzis[3], W-D.Apel[13], B.Asman[32], P.Astier[18], C.Astor Ferreres[30], J-E.Augustin[15], A.Augustinus[7], P.Baillon[7], P.Bambade[15], F.Barao[16], G.Barbiellini[34], D.Y.Bardin[12], A.Baroncelli[29], O.Barring[19], W.Bartl[37], M.J.Bates[25], M.Baubillier[18], K-H.Becks[39], C.J.Beeston[25], P.Beilliere[6], I.Belokopytov[31], P.Beltran[9], D.Benedic[8], J.M.Benlloch[36], M.Berggren[32], D.Bertrand[2], S.Biagi[17], F.Bianchi[33], J.H.Bibby[25], M.S.Bilenky[12], P.Billoir[18], J.Bjarne[19], D.Bloch[8], P.N.Bogolubov[12], D.Bollini[5], T.Bolognese[28], M.Bonapart[22], P.S.L.Booth[17], M.Boratav[18], P.Borgeaud[28], H.Borner[25], C.Bosio[29], O.Botner[35], B.Bouquet[15], M.Bozzo[10], S.Braibant[7], P.Branchini[29], K.D.Brand[39], R.A.Brenner[11], C.Bricman[2], R.C.A.Brown[7], N.Brummer[22], J-M.Brunet[6], L.Bugge[24], T.Buran[24], H.Burmeister[7], J.A.M.A.Buytaert[2], M.Caccia[20], M.Calvi[20], A.J.Camacho Rozas[30], J-E.Campagne[7], A.Campion[17], T.Camporesi[7], V.Canale[29], F.Cao[2], L.Carroll[17], C.Caso[10], E.Castelli[34], M.V.Castillo Gimenez[36], A.Cattai[7], F.R.Cavallo[5], L.Cerrito[29], P.Charpentier[7], P.Checchia[26], G.A.Chelkov[12], L.Chevalier[28], P.Chliapnikov[31], V.Chorowicz[18], R.Cirio[33], M.P.Clara[33], J.L.Contreras[36], R.Contri[10], G.Cosme[15], F.Couchot[15], H.B.Crawley[1], D.Crennell[27], M.Cresti[26], G.Crosetti[10], N.Crosland[25], M.Crozon[6], J.Cuevas Maestro[30], S.Czellar[11], S.Dagoret[15], E.Dahl-Jensen[21], B.Dalmagne[15], M.Dam[7], G.Damgaard[21], G.Darbo[10], E.Daubie[2], P.D.Dauncey[25], M.Davenport[7], P.David[18], A.De Angelis[34], M.De Beer[28], H.De Boeck[2], W.De Boer[13], C.De Clercq[2], M.D.M.De Fez Laso[36], N.De Groot[22], C.De La Vaissiere[18], B.De Lotto[34], A.De Min[20], C.Defoix[6], D.Delikaris[7], P.Delpierre[6], N.Demaria[33], L.Di Ciaccio[29], A.N.Diddens[22], H.Dijkstra[7], F.Djama[8], J.Dolbeau[6], O.Doll[39], K.Doroba[38], M.Dracos[8], J.Drees[39], M.Dris[23], W.Dulinski[8], R.Dzhelyadin[31], D.N.Edwards[17], L-O.Eek[35], P.A.-M.Eerola[11], T.Ekelof[35], G.Ekspong[32], J-P.Engel[8], V.Falaleev[31], A.Fenyuk[31], M.Fernandez Alonso[30], A.Ferrer[36], S.Ferroni[10], T.A.Filippas[23], A.Firestone[1], H.Foeth[7], E.Fokitis[23], F.Fontanelli[10], H.Forsbach[39], B.Franek[27], K.E.Fransson[35], P.Frenkiel[6], D.C.Fries[13], A.G.Frodesen[4], R.Fruhwirth[37], F.Fulda-Quenzer[15], H.Furstenau[13], J.Fuster[7], J.M.Gago[16], G.Galeazzi[26], D.Gamba[33], U.Gasparini[26], P.Gavillet[7], S.Gawne[17], E.N.Gazis[23], P.Giacomelli[5], K-W.Glitza[39], R.Gokieli[18], V.M.Golovatyuk[12], A.Goobar[32], G.Gopal[27], M.Gorski[38], V.Gracco[10], A.Grant[7], F.Grard[2], E.Graziani[29], M-H.Gros[15], G.Grosdidier[15], B.Grossetete[18], S.Gumenyuk[31], J.Guy[27], F.Hahn[39], M.Hahn[13], S.Haider[7], Z.Hajduk[22], A.Hakansson[19], A.Hallgren[35], K.Hamacher[39], G.Hamel De Monchenault[28], F.J.Harris[25], B.Heck[7], I.Herbst[39], J.J.Hernandez[36], P.Herquet[2], H.Herr[7], E.Higon[36], H.J.Hilke[7], S.D.Hodgson[25], T.Hofmokl[38], R.Holmes[1], S-O.Holmgren[32], J.E.Hooper[21], M.Houlden[17], J.Hrubec[37], P.O.Hulth[32], K.Hultqvist[32], D.Husson[8], B.D.Hyams[7], P.Ioannou[3], I.Ivanyushenkov[31], P-S.Iversen[4], J.N.Jackson[17], P.Jalocha[14], G.Jarlskog[19], P.Jarry[28], B.Jean-Marie[15], E.K.Johansson[32], M.Jonker[7], L.Jonsson[19], P.Juillot[8], R.B.Kadyrov[12], G.Kalkanis[3], G.Kalmus[27], G.Kantardjian[7], F.Kapusta[18], P.Kapusta[14], S.Katsanevas[3], E.C.Katsoufis[23], R.Keranen[11], J.Kesteman[2], B.A.Khomenko[12], B.King[17], N.J.Kjaer[21], H.Klein[7], W.Klempt[7], A.Klovning[4], P.Kluit[2], J.H.Koehne[13], B.Koene[22], P.Kokkinias[9], M.Kopf[13], M.Koratzinos[7], K.Korcyl[14], A.V.Korytov[12], B.Korzen[7], C.Kourkoumelis[3], T.Kreuzberger[37], J.Krolikowski[38], U.Kruener-Marquis[39], W.Krupinski[14], W.Kucewicz[20], K.Kurvinen[11], M.I.Laakso[11], C.Lambropoulos[9], J.W.Lamsa[1], L.Lanceri[34], V.Lapin[31], J-P.Laugier[28], R.Lauhakangas[11], P.Laurikainen[11], G.Leder[37], F.Ledroit[6], J.Lemonne[2], G.Lenzen[39], V.Lepeltier[15], A.Letessier-Selvon[18], E.Lieb[39], E.Lillestol[7], E.Lillethun[4], J.Lindgren[11], I.Lippi[26], R.Llosa[36], M.Lokajicek[12], J.G.Loken[25], M.A.Lopez Aguera[30], A.Lopez-Fernandez[15], D.Loukas[9], J.J.Lozano[36], R.Lucock[27], B.Lund-Jensen[35], P.Lutz[6], L.Lyons[25], G.Maehlum[7], N.Magnussen[39], J.Maillard[6], A.Maltezos[9], F.Mandl[37], J.Marco[30], J-C.Marin[7], A.Markou[9], L.Mathis[6], C.Matteuzzi[20], G.Matthiae[29], M.Mazzucato[26], M.Mc Cubbin[17], R.Mc Kay[1], E.Menichetti[33], C.Meroni[20], W.T.Meyer[1], W.A.Mitaroff[37], G.V.Mitselmakher[12], U.Mjoernmark[19], T.Moa[32], R.Moeller[21], K.Moenig[39], M.R.Monge[10], P.Morettini[10], H.Mueller[13], H.Muller[7], G.Myatt[25], F.Naraghi[18], U.Nau-Korzen[39], F.L.Navarria[5], P.Negri[20], B.S.Nielsen[21], V.Nikolaenko[31], V.Obraztsov[31], R.Orava[11], A.Ouraou[28], R.Pain[18], H.Palka[14], T.Papadopoulou[23], L.Pape[7], A.Passeri[29], M.Pegoraro[26], V.Perevozchikov[31], M.Pernicka[37], A.Perrotta[5], M.Pimenta[16], O.Pingot[2], C.Pinori[26], A.Pinsent[25], M.E.Pol[16], B.Poliakov[31], G.Polok[14], P.Poropat[34], P.Privitera[5], A.Pullia[20], J.Pyyhtia[11], A.A.Rademakers[22], D.Radojicic[25], S.Ragazzi[20], W.H.Range[17], P.N.Ratoff[25], A.L.Read[24], N.G.Redaelli[20], M.Regler[37], D.Reid[17], P.B.Renton[25], L.K.Resvanis[3], F.Richard[15], J.Ridky[12], G.Rinaudo[33], I.Roditi[7], A.Romero[33], P.Ronchese[26], E.I.Rosenberg[1], U.Rossi[5], E.Rosso[7], P.Roudeau[15], T.Rovelli[5], V.Ruhlmann[28], A.Ruiz[30], H.Saarikko[11], Y.Sacquin[28], E.Sanches[36], J.Sanches[36], E.Sanchis[36], M.Sannino[10], M.Schaeffer[8], H.Schneider[13], F.Scuri[34], A.Sebastia[36], A.M.Segar[25], R.Sekulin[27], M.Sessa[34], G.Sette[10], R.Seufert[13], R.C.Shellard[7], P.Siegrist[28], S.Simonetti[10], F.Simonetto[26], A.N.Sissakian[12], T.B.Skaali[24], J.Skeens[1], G.Skjevling[24], G.Smadja[28], G.R.Smith[27], R.Sosnowski[38], K.Spang[21], T.Spassoff[12], E.Spiriti[29], S.Squarcia[10], H.Staeck[39], C.Stanescu[29], G.Stavropoulos[9], F.Stichelbaut[2], A.Stocchi[20], J.Strauss[37],

R.Strub[8], C.J.Stubenrauch[7], M.Szczekowski[38], M.Szeptycka[38], P.Szymanski[38], S.Tavernier[2], O.Tchikilev[31], G.Theodosiou[9], A.Tilquin[6], J.Timmermans[22], V.G.Timofeev[12], L.G.Tkatchev[12], D.Z.Toet[22], A.K.Topphol[4], L.Tortora[29], M.T.Trainor[25], D.Treille[7], U.Trevisan[10], G.Tristram[6], C.Troncon[20], A.Tsirou[7], E.N.Tsyganov[12], M.Turala[14], R.Turchetta[8], M-L.Turluer[28], T.Tuuva[11], I.A.Tyapkin[12], M.Tyndel[27], S.Tzamarias[7], F.Udo[22], S.Ueberschaer[39], V.A.Uvarov[31], G.Valenti[5], E.Vallazza[33], J.A.Valls Ferrer[36], G.W.Van Apeldoorn[22], P.Van Dam[22], W.K.Van Doninck[2], N.Van Eijndhoven[7], C.Vander Velde[2], J.Varela[16], P.Vaz[16], G.Vegni[20], J.Velasco[36], L.Ventura[26], W.Venus[27], F.Verbeure[2], L.S.Vertogradov[12], L.Vibert[18], D.Vilanova[28], E.V.Vlasov[31], A.S.Vodopyanov[12], M.Vollmer[39], G.Voulgaris[3], M.Voutilainen[11], V.Vrba[12], H.Wahlen[39], C.Walck[32], F.Waldner[34], M.Wayne[1], A.Wehr[39], P.Weilhammer[7], J.Werner[39], A.M.Wetherell[7], J.H.Wickens[2], J.Wikne[24], G.R.Wilkinson[25], W.S.C.Williams[25], M.Winter[8], D.Wormald[24], G.Wormser[15], K.Woschnagg[35], N.Yamdagni[32], P.Yepes[22], A.Zaitsev[31], A.Zalewska[14], P.Zalewski[38], P.I.Zarubin[12], E.Zevgolatakos[9], G.Zhang[39], N.I.Zimin[12], R.Zitoun[18], R.Zukanovich Funchal[6], G.Zumerle[26], J.Zuniga[36]

[1] Ames Laboratory and Department of Physics, Iowa State University, Ames IA 50011, USA
[2] Physics Department, Univ. Instelling Antwerpen, Universiteitsplein 1, B-2610 Wilrijk, Belgium and IIHE, ULB-VUB, Pleinlaan 2, B-1050 Brussels, Belgium and Service de Phys. des Part. Elém., Faculté des Sciences, Université de l'Etat Mons, Av. Maistriau 19, B-7000 Mons, Belgium
[3] Physics Laboratory, University of Athens, Solonos Str. 104, GR-10680 Athens, Greece
[4] Department of Physics, University of Bergen, Allégaten 55, N-5007 Bergen, Norway
[5] Dipartimento di Fisica, Università di Bologna and INFN, Via Irnerio 46, I-40126 Bologna, Italy
[6] Collège de France, Lab. de Physique Corpusculaire, 11 pl. M. Berthelot, F-75231 Paris Cedex 05, France
[7] CERN, CH-1211 Geneva 23, Switzerland
[8] Division des Hautes Energies, CRN - Groupe DELPHI, B.P. 20 CRO, F-67037 Strasbourg Cedex, France
[9] Greek Atomic Energy Commission, Nucl. Research Centre Demokritos, P.O. Box 60228, GR-15310 Aghia Paraskevi, Greece
[10] Dipartimento di Fisica, Università di Genova and INFN, Via Dodecaneso 33, I-16146 Genova, Italy
[11] Dept. of High Energy Physics, University of Helsinki, Siltavuorenpenger 20 C, SF-00170 Helsinki 17, Finland
[12] Joint Institute for Nuclear Research, Dubna, Head Post Office, P.O. Box 79, 101 000 Moscow, USSR.
[13] Institut für Experimentelle Kernphysik, Universität Karlsruhe, Postfach 6980, D-7500 Karlsruhe 1, FRG
[14] High Energy Physics Laboratory, Institute of Nuclear Physics, Ul. Kawiory 26 a, PL-30055 Krakow 30, Poland
[15] Université de Paris-Sud, Lab. de l'Accélérateur Linéaire, Bat 200, F-91405 Orsay, France
[16] LIP, Av. Elias Garcia 14 - 1e, P-1000 Lisbon Codex, Portugal
[17] Department of Physics, University of Liverpool, P.O. Box 147, GB - Liverpool L69 3BX, UK
[18] LPNHE, Universités Paris VI et VII, Tour 33 (RdC), 4 place Jussieu, F-75230 Paris Cedex 05, France
[19] Department of Physics, University of Lund, Sölvegatan 14, S-22363 Lund, Sweden
[20] Dipartimento di Fisica, Università di Milano and INFN, Via Celoria 16, I-20133 Milan, Italy
[21] Niels Bohr Institute, Blegdamsvej 17, DK-2100 Copenhagen 0, Denmark
[22] NIKHEF-H, Postbus 41882, NL-1009 DB Amsterdam, The Netherlands
[23] National Technical University, Physics Department, Zografou Campus, GR-15773 Athens, Greece
[24] Physics Department, University of Oslo, Blindern, N-1000 Oslo 3, Norway
[25] Nuclear Physics Laboratory, University of Oxford, Keble Road, GB - Oxford OX1 3RH, UK
[26] Dipartimento di Fisica, Università di Padova and INFN, Via Marsolo 8, I-35131 Padua, Italy
[27] Rutherford Appleton Laboratory, Chilton, GB - Didcot OX11 OQX, UK
[28] CEN-Saclay, DPhPE, F-91191 Gif-sur-Yvette Cedex, France
[29] Istituto Superiore di Sanità, Ist. Naz. di Fisica Nucl. (INFN), Viale Regina Elena 299, I-00161 Rome, Italy and Dipartimento di Fisica, Università di Roma II and INFN, Tor Vergata, I-00173 Rome.
[30] Facultad de Ciencias, Universidad de Santander, av. de los Castros, E - 39005 Santander, Spain
[31] Inst. for High Energy Physics, Serpukow P.O. Box 35, Protvino, (Moscow Region), USSR.
[32] Institute of Physics, University of Stockholm, Vanadisvägen 9, S-113 46 Stockholm, Sweden
[33] Dipartimento di Fisica Sperimentale, Università di Torino and INFN, Via P. Giuria 1, I-10125 Turin, Italy
[34] Dipartimento di Fisica, Università di Trieste and INFN, Via A. Valerio 2, I-34127 Trieste, Italy and Istituto di Fisica, Università di Udine, I-33100 Udine, Italy
[35] Department of Radiation Sciences, University of Uppsala, P.O. Box 535, S-751 21 Uppsala, Sweden
[36] Inst. de Fisica Corpuscular IFIC, Centro Mixto Univ. de Valencia-CSIC, Avda. Dr. Moliner 50, E-46100 Burjassot (Valencia), Spain
[37] Institut für Hochenergiephysik, Österreich Akad. d. Wissensch., Nikolsdorfergasse 18, A-1050 Vienna, Austria
[38] Inst. Nuclear Studies and, University of Warsaw, Ul. Hoza 69, PL-00681 Warsaw, Poland
[39] Fachbereich Physik, University of Wuppertal, Postfach 100 127, D-5600 Wuppertal 1, FRG

1. *Introduction*

Results on charged particle multiplicity distributions in e^+e^- collisions[1]−[7] reveal interesting features. Among them are the rapid rise of the average charged multiplicity with increasing energy, the existence of forward-backward multiplicity correlations which are positive and almost energy independent and evidence for approximate KNO-scaling[8].

In this paper we report on properties of the charged particle multiplicity distributions from e^+e^- annihilation into hadrons studied in the DELPHI detector at LEP at center-of-mass energies, $\sqrt{s}$, between 91.0 and 91.5 GeV. We compare our results on multiplicity distributions of charged particles with those obtained in e^+e^- annihilation at lower energies, as well as with the expectations of the Lund Parton Shower model and other phenomenological models. Since our data are recorded at a much higher energy than those in earlier studies, it is of special interest to study the KNO-scaling properties and also the forward-backward multiplicity correlations.

In section 2 we briefly describe the DELPHI detector and discuss our event sample, selection criteria, correction procedure and treatment of systematic errors. Experimental results on the charged multiplicities are presented in section 3 and on the forward-backward multiplicity correlations in section 4. Section 5 summarizes our conclusions.

2. *Data Selection*

The data were recorded with the DELPHI detector at the CERN e^+e^- collider LEP. In the present paper a sample of 47400 events with $n_{ch}\geq 5$ was used. A detailed description of the detector, of the trigger conditions and of the analysis chain can be found in ref. [9]. Here only the specific properties relevant to the following analysis are summarized.

Charged particles were measured in the Time Projection Chamber (TPC) as described in more detail in our previous paper[10] on global event shape distributions in the hadronic decays of the Z^0. Up to 16 space points in the TPC were used for track reconstruction by the DELPHI analysis package, DELANA[11]. The momentum resolution was found to be $\delta p/p^2 = \pm 0.012(GeV/c)^{-1}$. Points on neighbouring tracks could be distinguished only if they were separated by at least 15 mm in z, the coordinate along the beam axis, and in $r\phi$, the azimuthal coordinate. No differences in track-finding efficiency were observed between the data and the Monte Carlo simulation.

The tracks of charged particles were retained only if:

(a) they extrapolated back to within 5 cm of the beam axis in r and to within 10 cm of the nominal crossing point in z,

(b) their momentum p was larger than 0.1 GeV/c,

(c) their measured track length was above 50 cm,

(d) their polar angle θ was between 25° and 155°.

Hadronic events were then selected by requiring that:

(a) the total energy of charged particles $E_{ch} = \sum_i E_i$ in each of the two hemispheres defined with respect to the beam axis exceeded 3 GeV, where E_i were the particle energies (assuming π mass),

(b) the total energy of charged particles seen in both hemispheres together exceeded 15 GeV,

(c) there were at least 5 charged particles with momenta above 0.2 GeV/c,

(d) the polar angle θ of the sphericity axis was in the range $50° < \theta < 130°$.

The resulting data sample comprised 25364 events. The last cut ensured that the retained events were well contained inside the TPC. After all four cuts, events due to beam-gas scattering and to $\gamma\gamma$ interactions were reduced to below 0.1% of the sample. The largest background was due to $\tau^+\tau^-$ events. From the Monte Carlo simulation this was calculated to be 0.15% of the sample.

The multiplicity distributions presented below are the result of correcting the raw data for limited geometrical acceptance and resolution of the TPC, limited efficiency of the track finding, particle interactions in the material of the detector, other detector imperfections, applied kinematical cuts, and also for QED initial state radiation. Like in our previous paper[10], the correction procedure was based on 50000 Monte Carlo events generated according to the Lund Parton Shower (PS) (Monte Carlo program JETSET version 6.3) model[12],[13]. Correction factors were obtained by comparing the ("true") distributions at the beginning of the simulation with the ("observed") distributions after reconstruction and selection. The "true" distributions were constructed from the final state particles of lifetime above 10^{-9} s which had not yet been tracked through the detector. The events were generated without initial state radiation. The charged particles from K^0_s and Λ decays were included, irrespective of how far away from the interaction point the decay occured, while the charged particles from K^0_L decay were not included. The "observed" distributions were constructed from the final state particles observed after tracking events, generated with initial state radiation, through the DELPHI detector to produce simulated raw data which were then processed through the same reconstruction and analysis programs as the real data.

The corrected multiplicity distribution was determined by unfolding the observed multiplicity distribution. Let $N_{obs}(n_{obs})$ be the number of accepted events with n_{obs} accepted charged tracks and $N_{tr}(n_{tr})$ be the corrected number of events with n_{tr} ($n_{tr} = even$) produced charged particles. The two distributions are related by the matrices M_1 and M_2:

$$N_{tr}(n_{tr}) = \sum_{n_{obs}} M_1(n_{tr}, n_{obs}) N_{obs}(n_{obs}), \tag{1}$$

$$N_{obs}(n_{obs}) = \sum_{n_{tr}} M_2(n_{obs}, n_{tr}) N_{tr}(n_{tr}) \tag{2}$$

with coefficients $M_1(n_{tr}, n_{obs})$ and $M_2(n_{obs}, n_{tr})$ determined using Monte Carlo events generated according to the Lund PS model. The matrix M_1 in (1) was used for the determination of the corrected multiplicity distributions. The matrix M_2 in (2) was used for the transformation of the multiplicity distributions predicted by models in order to compare them with the observed multiplicity distribution and calculate the corresponding χ^2. The matrix M_2 is straightforward to construct and is independent of the multiplicity distribution of the model used in the Monte Carlo simulation, but strongly dependent of the detector respons as is desired. There is only a weak dependence on the kinematic variables generated by the model. The matrix M_1 is not taken as the inverse of M_2 since that would give rise to instabilities. It is therefore constructed from a preknowledge of the shape of the multiplicity distribution. Once a model has been tested using (2) and found to well represent the raw data, i.e. $N_{obs}(n_{obs})$, this model can be used in constructing the matrix M_1. Note that the reconstructed numbers of events

with $n_{tr} \leq 8$ are strongly model dependent in such a correction procedure.

The above procedure was applied to the multiplicity distribution in the full phase space and in the single hemisphere defined by the plane perpendicular to the sphericity axis.

The appropriate correction formalism for the analysis of forward-backward multiplicity correlations is a simple extension of formula (1) so the corrected two-dimensional multiplicity distribution reads:

$$N_{tr}(n_{F,tr},n_{B,tr}) = \sum_{n_{F,obs},n_{B,obs}} M(n_{F,tr},n_{B,tr},n_{F,obs},n_{B,obs}) N_{obs}(n_{F,obs},n_{B,obs}), \qquad (3)$$

where n_F and n_B are the numbers of particles produced in the forward and backward hemispheres with respect to the sphericity axis. Since for e^+e^- collisions there is no difference between the "forward" and "backward" hemispheres, each event was entered twice.

Contributions to systematic errors arise from possible differences between the actual detector performance and that represented in the simulation program. To evaluate these, we tested the effects of a range of possible differences in the Monte Carlo simulation, such as additional momentum smearing, a constant sagitta shift and a different drift velocity inside the TPC. We also varied our selection criteria over a wide range. The matrices $M_1(n_{tr},n_{obs})$, $M_2(n_{obs},n_{tr})$ and $M(n_{F,tr},n_{B,tr},n_{F,obs},n_{B,obs})$ were also evaluated using the Marchesini-Webber PS model[14] and the Lund Matrix Element (ME) (Monte Carlo program JETSET version 7.2) model[15],[13] with parameters optimized at $\sqrt{s} = 91$ GeV[16]. The variance of the M values computed from the three different models[1] was taken as one contribution to the systematic uncertainty.

3. *Full Phase Space and Single Hemisphere Charged Multiplicity Distributions*

The charged multiplicity distribution for the raw data is shown in Table 1. The corrected charged particle multiplicity distributions for full phase space and single hemisphere are presented in Table 2 and shown in Fig.1. The average charged multiplicity $<n_{ch}>$, the dispersion $D = (<n_{ch}^2> - <n_{ch}>^2)^{1/2}$, the ratio $<n_{ch}>/D$ and the normalized moments $C_l = <n_{ch}^l>/<n_{ch}>^l$ for both distributions are given in Table 3. The quoted errors are calculated from the statistical errors and from the correction procedure. The values of $<n_{ch}>$ and D in Table 3 are reduced by 2% due to a correction for electrons from photon conversions before the TPC which are not accounted for in the Monte Carlo. This correction was not applied to the multiplicity distributions given in Table 2. We take this 2% into account as additional systematic uncertainty.

Our value of the average charged multiplicity $<n_{ch}> = 20.71 \pm 0.04(stat) \pm 0.77(syst)$ agrees well with the previous value of DELPHI[10] and with those corrected values $<n_{ch}>$ at $\sqrt{s} = 91$ GeV presented by ALEPH[17], MARK2[18] and OPAL[19]. The values of $<n_{ch}>$ measured by DELPHI and by other e^+e^- experiments [1]−[7],[17]−[19] are shown in Fig.2. For all of the e^+e^- data shown in Fig.2 and used in the following fits, the average multiplicity value includes the charged secondaries of K^0_s, Λ and $\bar{\Lambda}$ decays.

The fits to our values of $<n_{ch}>$ and other available e^+e^- data[1]−[7], [17]−[19] as a function of energy using various parametrizations give results which are not very different from those obtained

---

[1] The variance for optimized Lund ME is smaller then for untuned standard Lund ME.

recently by TASSO[1] at lower energy. We find:

– for $< n_{ch} > = a + b \cdot ln(s) + c \cdot \ln^2(s)$:

$a = 3.320 \pm 0.083$, $b = -0.408 \pm 0.055$, $c = 0.263 \pm 0.008$ with $\chi^2/NDF = 79/69$;

– for $< n_{ch} > = a \cdot s^b$:

$a = 2.228 \pm 0.026$, $b = 0.249 \pm 0.002$ with $\chi^2/NDF = 153/70$;

– for $< n_{ch} > = a + b \cdot exp(c\sqrt{ln(s/Q_0^2)})$ at $Q_0^2 = 1$ GeV^2:

$a = 2.527 \pm 0.072$, $b = 0.094 \pm 0.010$, $c = 1.775 \pm 0.038$ with $\chi^2/NDF = 92/69$.[2]

One sees that with the new LEP data it is now possible to exclude the power law dependence $< n_{ch} > = a \cdot s^b$.

We have also fitted the data presented in Fig.2 in the energy range from 10 to 91 GeV to the form

$$< n_{ch} > = a \cdot \alpha_s^b \cdot exp(c/\sqrt{\alpha_s})(1 + O(\sqrt{\alpha_s})) \tag{4}$$

which was obtained in ref. [20],[21] on a basis of QCD in the next-to-leading order. The running coupling constant in (4) was taken as

$$\frac{\alpha_s(s)}{4\pi} = \frac{1}{\beta_0 ln(s/\Lambda^2)} - \frac{\beta_1 lnln(s/\Lambda^2)}{\beta_0^3 \ln^2(s/\Lambda^2)}. \tag{5}$$

Here a is a normalization constant and the parameters β_0, β_1, b and c are fixed at the values $\beta_0 = 11 - 2N_f/3 = 7.67$, $\beta_1 = 102 - 38N_f/3 = 38.67$, $b = 1/4 + (10N_f)/(27\beta_0) = 0.49$ and $c = \sqrt{96\pi}/\beta_0 = 2.27$ for $N_f = 5$[21]. According to ref. [21] one can neglect the $O(\sqrt{\alpha_s})$ term in (4) and treat a and Λ as free parameters. The fit (shown by the dash-dotted curve in Fig.2) gives very good agreement with the data ($\chi^2/NDF = 2.3/11$). The best values of the parameters are $a = 0.066 \pm 0.013$ and $\Lambda = 138 \pm 62$ MeV. As explained in ref. [21], Λ is a process-dependent quantity not necessarily equal to $\Lambda_{\overline{MS}}$. However it is expected to be close to $\Lambda_{\overline{MS}}$ if the $O(\sqrt{\alpha_s})$ correction does turn out to be small.

From Fig.1 (dashed curves) and Fig.2 (continuous curve) one sees that the Lund PS (JETSET 6.3) model[12],[13] describes the e^+e^- data reasonably well. The fits to the raw multiplicity data of the Lund PS model, transformed according to (2) for detector respons, are reasonably good, giving $\chi^2/NDF = 64/36$ for full phase space and $\chi^2/NDF = 47/25$ for single hemisphere.[3] These results are of interest in view of the physics content of the Lund PS model[22],[23], [12],[13]. The model contains three separate phases. First, there is the hard scattering phase, treated perturbatively, during

---

[2] With the parameter c fixed at the value $c = \sqrt{72/(33 - 2N_f)}$, the number of flavours N_f chosen equal to the TASSO values[1] and Q_0 free, we obtain $a = 2.122 \pm 0.134$, $b = 0.049 \pm 0.009$, $Q_0 = 0.306 \pm 0.098$ GeV with $\chi^2/NDF = 51/69$.

[3] Although χ^2 contains not only statistical errors we consider a fit with a χ^2-probability larger than 0.1% as acceptable.

which parton showers develop in QCD branching processes (quark bremsstrahlung, gluon bremsstrahlung and quark pair production). These processes are cut-off at a virtuality of Q_0 = 1 GeV. The subsequent phase treats the non-perturbative, soft processes according to the Lund string fragmentation model, which transforms the multiparton state created by the first phase into hadrons. Finally, resonances and shortlived particles are allowed to decay into the final state particles, which correspond to the ones available for observation. At low c.m. energies the soft processes are dominating, whereas at such high energy as the one under present study the multiplicity fluctuations are mainly controlled by the hard processes. It is therefore of great interest to note that the model is able to describe the data reasonably well without any tuning of parameters.

The ratio $< n_{ch} > /D$ for the full phase space multiplicity distribution is shown as a function of energy in Fig.3.[4] It is energy independent, within the statistical and systematic errors. The ratio of $< n_{ch} > /D$ for full phase space to that for single hemisphere is $1.34 \pm 0.01 \pm 0.04$ for the DELPHI data and it too is energy independent. Indeed TASSO[1] gives for this ratio: 1.35 ± 0.03, 1.35 ± 0.03, 1.34 ± 0.01 and 1.35 ± 0.02 at 14, 22, 34.8 and 43.6 GeV, respectively. All these values are lower than the value of $\sqrt{2}$ expected for two-jet events, if the jets are produced independently, as predicted in some phenomenological approaches[24] for the high LEP energies. The predictions of the Lund PS model agree well with the DELPHI values of $< n_{ch} > /D$ for full phase space and single hemisphere distributions, the Lund PS model giving 3.39 ± 0.01 and 2.47 ± 0.01, respectively.

Energy independence of the ratio $< n_{ch} > /D$ suggests a KNO-scaling property[8] of the multiplicity distribution. KNO-scaling implies an energy independence of the normalized moments C_q (we recall that $< n_{ch} > /D = (C_2 - 1)^{-1/2}$) and of the function $\psi(z) = < n_{ch} > P(n_{ch})$ plotted versus a variable $z = n_{ch} / < n_{ch} >$. The normalized moments of the full phase space and single hemisphere distributions are shown as functions of c.m. energy in Fig.4. There is no indication of an energy variation of C_2 to C_5 for c.m. energies larger than about 20 GeV. The KNO-functions $\psi(z)$ for the DELPHI and lower energy data starting from $\sqrt{s} = 14$ GeV are shown in Fig.5. They also support approximate scaling.[5]

In the Lund model, which generally agrees well with data at all energies in the presently available range of energies, the hard processes tend to broaden the multiplicity distribution in terms of the KNO-variable z as the energy is increased, whereas the soft processes lead to a narrowing (since it is almost Poissonian at fixed number of partons). The two opposing trends combine in such a way that an approximate KNO-scaling holds. At least the $D / < n >$ ratio remains almost constant in the energy range $15 - 1000$ GeV[25]. The trend seen in ref. [25] indicates a broadening in the z-variable at energies much beyond 1 TeV and this is further supported by Lund model simulations made at very high energies[26]. Also it has been proven[27] – [30] that a broad class of branching processes exibit KNO-like scaling. All this agrees with the experimental observation of approximate KNO-scaling in the energy interval from 20 GeV to 91 GeV. Notice, however, that based on the geometrical model of multiparticle production Chou and Yang[31] expect in e^+e^- a Poisson distribution and thus no KNO-scaling. Their statement is strictly limited to two-jet events.

Successful fits of the Negative Binomial (NB) distribution have been made to data at lower energies. Reasonably good agreements have also been obtained to simulated data from the Lund model[26] at low as well as very high energies. The fit to our data by the NB distribution[6]

---

[4] The PLUTO points here and elsewhere are taken from ref. [1]

[5] Note that the DELPHI points at the two smallest z values corresponding to multiplicities $n \lesssim 8$ are strongly affected by the correction procedure and should be treated with caution.

[6] In the NB fit to the multiplicity distribution for the full phase space we used the normalized even component of the NB.

$$P_n(m,k)=\frac{k(k+1)...(k+n-1)}{n!(1+m)^k}(\frac{m}{1+m})^n, \tag{6}$$

where m and k are positive parameters and $m=<n>/k$, gives $k^{-1}=0.0411\pm 0.0012$, $m=0.879\pm 0.025$ with $\chi^2/NDF=80/34$ for the full phase space and $k^{-1}=0.0664\pm 0.0017$, $m=0.705\pm 0.017$ with $\chi^2/NDF=66/23$ for the single hemisphere.[7] The NB distribution (solid curves in Fig.1b,d) describes the data, but less successfully than the Lund PS model. Better agreement with the data is obtained for the Modified Negative Binomial (MNB) distribution[32], characterized by the generating function

$$M(x)=(\frac{1+\Delta(1-x)}{1+m(1-x)})^k, \tag{7}$$

where $m=\Delta+<n>/k$, with three fitted parameters $k=7.92\pm 0.31$, $m=0.644\pm 0.028$, $\Delta=-0.696\pm 0.024$ with $\chi^2/NDF=43/33$ for the full phase space[8] and $k=6.38\pm 0.26$, $m=1.172\pm 0.035$, $\Delta=-0.483\pm 0.035$ with $\chi^2/NDF=59/22$ for a single hemispere. These fits are shown by the histograms in Fig.1a,c.

The NB parameter k^{-1} for the multiplicity distribution in full phase space measured by DELPHI is compared with those at lower energies[1],[7] in Fig.6. A phenomenological fit of the form

$$k^{-1}=a+b\cdot ln(\sqrt{s}/Q_0) \tag{8}$$

(with $Q_0=1$ GeV) gives $a=-0.063\pm 0.005$ and $b=0.023\pm 0.002$ with $\chi^2/NDF=2.2/3$ (the HRS value of the k^{-1} given in ref. [7] without error and not consistent with the trend of other data has not been used in the fit). In the same Fig.6 we also show the recent EMC Collaboration data[34] on k^{-1} for μ^+p interactions versus total hadronic energy W. Fitting them to the form $k^{-1}=a+b\cdot ln(W/Q_0)$ we obtain $a=-0.133\pm 0.007$, and $b=0.050\pm 0.003$ with $\chi^2/NDF=6.6/6$. For $pp(\bar{p}p)$ data over the c.m. energy range from 10 to 900 GeV, the UA5 Collaboration obtained $a=-0.104\pm 0.004$ and $b=0.058\pm 0.001$[35]. Thus the slopes b for $pp(\bar{p}p)$ and μ^+p data are close to each other but significantly higher than for e^+e^- collisions.[9]

We have also compared the multiplicity distribution with the model of Ellis, Karliner and Kowalski[37] based on the idea that near-mass-shell ("cool") partons produced by conventional perturbative QCD showering break chiral symmetry spontaneously and independently when they convert non-perturbatively into hadrons. The average charged multiplicity $<n_{ch}>=21.9$ predicted by Ellis et al. for all events agrees with experiment. Their predictions $<n_{ch}>=31.5(20.5)$ for events with sphericity S above and below 0.15 can be compared with the corresponding measured values of $26.8\pm 0.1\pm 0.8$ ($19.7\pm 0.1\pm 0.6$). Although the data reflect the predicted trend towards higher multiplicity in higher sphericity events, the model is quantitatively unaccurate. Moreover the charged multi-

---

[7] This and all other parametrizations of multiplicity distribution were fitted to the observed data using the relation (2). In these fits the systematic uncertainty was taken into account and the bins on the tails of observed distributions were combined.

[8] We fitted the distribution of negatively charged particles following the arguments of R.Szwed, G.Wrochna and A.K.Wroblewski[33].

[9] A significantly larger slope value $b=0.046\pm 0.002$ for e^+e^- collisions obtained earlier[36] and used by the EMC Collaboration[34] is based on the fit to the less precise e^+e^- data at lower energy.

plicity distribution obtained in the model using all links in a triangulation of space with "cool" partons as vertices is significantly broader than the data.

4. *Forward-Backward Multiplicity Correlations*

To study the correlations between particles produced in the different c.m.s. hemispheres, forward (F) and backward (B), one measures the average charged multiplicity in one hemisphere as a function of the charged multiplicity in the opposite one, $< n_F >$ versus n_B, or vice versa. Correlations are usually parametrized as

$$< n_F > = a + b \cdot n_B, \tag{9}$$

where b measures the correlation strength. In hadron-hadron collisions, clear evidence exists for strong F-B correlations with b rising with increasing energy as $ln(s)$ (see, for example ref. [38] and refs. therein). New precise TASSO data have established weak, positive and approximately energy independent F-B correlations from $\sqrt{s} = 14$ GeV to 46.8 GeV[1]. However the HRS Collaboration with their high statistics data at $\sqrt{s} = 29$ GeV[7],[39] sees no evidence for correlations (see Table 4).

The variation of $< n_F >$ with n_B measured by DELPHI is shown in Fig.7a. In agreement with TASSO [1], but contrary to the HRS results[7],[39], we find a slow rise of $< n_F >$ with increasing n_B. The fit of the form (9) (straight line in Fig.7a) gives the values $b = 0.118 \pm 0.009$ with $\chi^2/NDF = 25/23$. As one can see from Fig.7a, the Lund PS model provides a good description of the data. Fitting the Lund PS model points gives $b = 0.091 \pm 0.004$ and $\chi^2/NDF = 42/23$. Our value of the correlation strength parameter b when compared with the TASSO values (see Table 4, second column) exhibits, within errors, no energy variation from $\sqrt{s} = 14$ GeV to 91 GeV.

We find that the F-B correlations are strongest in the central region, defined by the c.m. rapidity cut $|y| \leq 1$.[10] The dependence of $< n_F >$ on n_B for this region is also shown in Fig.7b. The fit of the form (9) (straight line in Fig.7b) gives in this case: $b = 0.289 \pm 0.012$ with $\chi^2/NDF = 28/14$. The Lund PS model is again well consistent with the data. Outside the central region, i.e. for $|y| > 1$, the correlations are small; the fit gives $b = 0.057 \pm 0.008$ with $\chi^2/NDF = 14/16$.

We also find, in agreement with earlier results of the NA22[38] and TASSO[1] Collaborations, that the F-B correlations are dominated by the correlations between unlike sign $(+-)$ charged particles. This is clearly seen from Fig.8, where we show the dependence of $< n_F >$ on n_B for the unlike sign and like sign $(++$ or $--)$ particles together with the results of fits of the form (9) (straight lines) and the Lund PS model predictions. For unlike sign particles $b = 0.177 \pm 0.009$. Table 4 (third column) shows that this parameter decreases with increasing energy. For like sign particles, the correlation strength $b = 0.020 \pm 0.006$ is significantly smaller (the Lund PS model gives $b = 0.009 \pm 0.003$). Applying the rapidity cut $|y| \leq 1$ for unlike and like sign particles gives $b = 0.350 \pm 0.015$ and $b = 0.210 \pm 0.013$, respectively.

5. *Summary and Conclusions*

In the present paper, the charged particle multiplicity distributions at $\sqrt{s} = 91$ GeV measured in the DELPHI experiment at LEP have been analysed. Our main conclusions based on 25364 events after the cuts, can be summarized as follows:

---

[10] In calculating the rapidity $y = 1/2 ln((E + p_L)/(E - p_L))$, the p_L was taken as the momentum component parallel to the sphericity axis, and the pion mass was assigned to all particles.

– The average charged particle multiplicity is $< n_{ch} > = 20.71 \pm 0.04(stat) \pm 0.77(syst)$ and the dispersion $D = 6.28 \pm 0.03(stat) \pm 0.43(syst)$.

– The Lund Parton Shower model describes all of the studied features of the charged particle multiplicity distributions at $\sqrt{s} = 91$ GeV.

– Forward-backward correlations exist in e^+e^- collisions at $\sqrt{s} = 91$ GeV. They are positive, strongest in the central $|y| < 1$ region and larger for the particles of opposite charge.

– The charged multiplicity distributions for full phase space and single hemisphere are described by the Negative Binomial and Modified Negative Binomial distributions. The energy dependence of the NB parameter k^{-1} for e^+e^- collisions can be parametrized by the form (8), but with a slope value only half that for μ^+p and $pp(\bar{p}p)$ collisions.

When further comparing the DELPHI results with those at lower energies, we conclude:

– The energy dependence of the average charged multiplicity for e^+e^- collisions is well described by the parametrizations $< n_{ch} > = a + b \cdot ln(s) + c \cdot \ln^2(s)$ and $< n_{ch} > = a + b \cdot exp(c\sqrt{ln(s/Q_0^2)})$, suggested respectively by the analysis of $pp(\bar{p}p)$ data and by QCD. The power law $< n_{ch} > = a \cdot s^b$ suggested by the hydrodynamical models is practically excluded. The expression $< n_{ch} > = a \cdot \alpha_s^b \cdot exp(c/\sqrt{\alpha_s})$ with the running coupling constant $\alpha_s(s)$ in the form (5) deduced on a basis of QCD in next-to-leading order describes the data very well; the best value of the process-dependent QCD parameter Λ is 138 ± 62 MeV.

– The charged multiplicity distribution for e^+e^- collisions from $\sqrt{s} \approx 20$ to 91 GeV shows approximate KNO-scaling. This is seen from the energy independence of the normalised moments $C_2 - C_5$ and of the KNO-function $\psi(z)$.

After this paper was ready for publication we received an AMY Preprint[40] which reaches similar conclusion in KNO-scaling.

Acknowledgement

We are greatly indebted to our technical staffs and collaborators and funding agencies for their support in building the DELPHI detector and to the members of the SL Division for the speedy commissioning and superb performance of the LEP collider.

References

1. *TASSO Collaboration, W.Braunschweig et al.,* Z.Phys.C45(1989)193.

2. *ADONE Collaboration, C.Bacci et al.,* Phys.Lett.B86(1979)234.

3. *LENA Collaboration, B.Niczyporuk et al.,* Z.Phys.C9(1981)1.

4. *MARK1 Collaboration, J.L.Siegrist et al.,* Phys.Rev.D26(1982)969.

5. *CLEO Collaboration, M.S.Alam et al.,* Phys.Rev.Lett.49(1982)357.

6. *JADE Collaboration, W.Bartel et al.,* Z.Phys.C20(1983)187.

7. *HRS Collaboration, M.Derrick et al.,* Phys.Rev.D34(1986)3304.

8. *Z.Koba, H.B.Nielsen and P.Olesen,* Nucl.Phys.B40(1972)317.

9. *DELPHI Collaboration, P.Aarnio et al.,* Phys.Lett.B231(1989)539; *The DELPHI Detector at LEP*, CERN/EF 90-5, submitted to Nucl.Instr.Meth.

10. *DELPHI Collaboration, P.Aarnio et al.,* Phys.Lett.B240(1990)271.

11. *DELPHI Collaboration, DELPHI Data Analysis Program – User's Guide,* DELPHI Note 89-44 (1989), unpublished.

12. *M.Bengtsson and T.Sjostrand,* Phys.Lett.B185(1987)435.

13. *T.Sjostrand and M.Bengtsson,* Comp.Phys.Comm.43(1987)367.

14. *G.Marchesini and B.R.Webber,* Nucl.Phys.B238(1984)1.

15. *T.Sjostrand,* Comp.Phys.Comm.27(1982)243; ibid.28(1983)229.

16. *W.de Boer, H.Furstenau and J.H.Kohne,* IEKP-KA/90-4, to be published in Z.Phys.C.

17. *ALEPH Collaboration, D.Decamp et al.,* Phys.Lett.B234(1990)209.

18. *MARK2 Collaboration, G.S.Abrams et al.,* Phys.Rev.Lett.64(1990)1334.

19. *OPAL Collaboration, M.Z.Akrawy et al.,* Z.Phys.C47(1990)505.

20. *A.H.Mueller,* Nucl.Phys.B213(1983)85; ibid.B228(1983)351; ibid.B241(1984)141; *Yu.L.Dokshitzer and S.I.Troyan,* Preprint LNPI-922, Leningrad, 1984.

21. *B.R.Webber,* Phys.Lett.B143(1984)501.

22. *B.Andersson, G.Gustafson, G.Ingelman and T.Sjostrand,* Phys.Rep.97(1983)31.

23. *T.Sjostrand,* Nucl.Phys.B248(1984)469; Comp.Phys.Comm.39(1986)367.

24. *S.Barshay, Possibility of Observable New Behaviour for Multiparticle Production in e^+e^- Annihilation at LEP,* Preprint of Physikalisches Institute, Aachen, 1990.

25. *B.Andersson, P.Dahlqvist and G.Gustafson,* Z.Phys.C44(1989)455.

26. *T.Sjostrand,* Multiparticle Dynamics, Festschrift for Leon Van Hove and Proceedings, p.283. (Ed. A.Giovannini and W.Kittel), (World Scientific, 1990).

27. *A.M.Polyakov,* Sov.Phys.JETP 32(1971)296.

28. *Yu.L.Dokshitzer, V.A.Khoze and S.I.Troyan,* In Perturbative Quantum Chromodynamics, ed. A.H.Mueller, World Scientific, Singapore (1989), p.241.

29. *P.V.Chliapnikov and O.G.Tchikilev,* Phys.Lett.B235(1990)347.

30. *R.Szwed, G.Wrochna and A.K.Wroblewski,* Warsaw Univ. Preprint IFD/1/1990.

31. *T.T.Chou and Chen Ning Yang,* Phys.Rev.Lett.55(1985)1359; Phys.Lett.B167(1986)453; ibid.B171(1986)486.

32. *P.V.Chliapnikov and O.G.Tchikilev,* Phys.Lett.B242(1990)275.

33. *R.Szwed, G.Wrochna and A.K.Wroblewski,* Acta Phys.Polonica B19(1988)763.

34. *EMC Collaboration, M.Arneodo et al.,* Z.Phys.C35(1987)335.

35. *UA5 Collaboration, G.J.Alner et al.,* Phys.Lett.B167(1986)476.

36. *NA22 Collaboration, M.Adamus et al.,* Z.Phys.C32(1986)475.

37. *J.Ellis, M.Karliner and H.Kowalski,* Phys.Lett.B235(1990)341.

38. *NA22 Collaboration, V.V.Aivazyan et al.,* Z.Phys.C42(1989)533.

39. *HRS Collaboration, M.Derrick et al.,* Z.Phys.C35(1987)323.

40. *AMY Collaboration, H.W.Zheng et al.,* KEK Preprint 90-5.

Table 1:

The charged particle multiplicity distribution for the raw data in the full phase space.

no. charged particles	no. events
5	46
6	93
7	180
8	291
9	507
10	717
11	1026
12	1300
13	1527
14	1728
15	1855
16	1834
17	1829
18	1717
19	1644
20	1485
21	1292
22	1107
23	1053
24	822
25	666
26	572
27	459
28	380
29	293
30	250
31	201
32	129
33	116
34	74
35	51
36	43
37	19
38	13
39	13
40	7
41	6
42	7
43	3
44	3
45	3
47	2
51	1

Table 2:

Charged particle multiplicity distributions $P(n) = \frac{1}{N}\frac{dN}{dn}$ (%) for full phase space and single hemisphere. Errors include systematics. The 2% correction for excess electrons from photon conversions is not included.

n	P(n) (full phase space)	n	P(n) (single hemisphere)
2	(0.001±0.001)[1)]	1	0.124±0.020
4	(0.025±0.008)[1)]	2	0.466±0.065
6	0.155±0.040	3	1.21±0.17
8	0.674±0.055	4	2.67±0.10
10	2.28±0.16	5	4.56±0.17
12	4.85±0.28	6	7.04±0.26
14	8.22±0.44	7	8.58±0.31
16	11.10±0.58	8	9.97±0.36
18	12.90±0.66	9	10.20±0.36
20	13.10±0.67	10	9.87±0.35
22	11.70±0.60	11	8.85±0.32
24	9.79±0.51	12	7.83±0.28
26	7.53±0.40	13	6.44±0.23
28	5.76±0.31	14	5.19±0.19
30	4.14±0.23	15	4.14±0.15
32	2.93±0.17	16	3.22±0.12
34	1.88±0.11	17	2.490±0.094
36	1.220±0.080	18	1.980±0.077
38	0.755±0.056	19	1.400±0.056
40	0.478±0.100	20	1.040±0.140
42	0.251±0.060	21	0.760±0.100
44	0.143±0.035	22	0.591±0.081
46	0.082±0.021	23	0.426±0.059
48	0.020±0.006	24	0.285±0.040
50	0.011±0.017	25	0.212±0.031
52	0.006±0.005	26	0.128±0.019
		27	0.076±0.014
		28	0.041±0.007
		29	0.042±0.021
		30	0.015±0.007
		31	0.015±0.005
		32	0.007±0.001
		33	0.003±0.001
		34	0.006±0.007

[1)] Not measured, taken from the Lund PS model.

Table 3:

Moments for full phase space and single hemisphere charged particle multiplicity distributions. The first error is statistical, the second is systematic.

Moment	Full phase space	Single hemisphere
<n>	20.71±0.04±0.77	10.35±0.02±0.47
D	6.28±0.03±0.43	4.19±0.02±0.32
<n>/D	3.30±0.02±0.20	2.47±0.01±0.20
C_2	1.092±0.003±0.03	1.164±0.003±0.03
C_3	1.293±0.003±0.03	1.544±0.006±0.04
C_4	1.647±0.009±0.04	2.296±0.018±0.06
C_5	2.245±0.017±0.06	3.770±0.051±0.09

Table 4:

Fitted values of the correlation strength parameter b in $\langle n_F \rangle = a + b \cdot n_B$ for all and for unlike sign charged particles obtained by TASSO[1], HRS[7],[39] and in the present experiment.

√s (GeV)		b (all particles)	b (unlike sign particles)
TASSO	14.0	0.085±0.014	0.306±0.010
TASSO	22.0	0.084±0.016	0.251±0.013
HRS	29.0	-0.001±0.015	
TASSO	34.8	0.089±0.003	0.226±0.003
TASSO	43.6	0.111±0.009	0.200±0.009
DELPHI	91.0	0.118±0.009	0.177±0.009

Figure Captions

Fig.1 Corrected charged particle multiplicity distributions (full dots) for a,b) full phase space and c,d) single hemisphere compared with the Lund PS (JETSET 6.3) model predictions (b,d, dashed curves), with the fits to the NB distribution (b,d, solid curves) and to the Modified NB distribution[32] (a,c, histograms).

Fig.2 Energy dependence of the average charged particle multiplicity in e^+e^- collisions. The data at lower energies are taken from refs. [1]−[7],[17]−[19]. Solid curve is the prediction of the Lund PS (JETSET 6.3). Dash-dotted curve is the result of the fit to the QCD-inspired formula (4) (see the text).

Fig.3 Energy dependence of $< n_{ch} > /D$ measured by DELPHI, TASSO[1], HRS[7] and PLUTO (the PLUTO points are taken from ref. [1]). The DELPHI and TASSO points are shown with their systematic and statistical errors.

Fig.4 Energy dependence of the normalized moments C_l for a) full phase space and b) single hemisphere multiplicity distributions measured by DELPHI, TASSO[1], HRS[7] and PLUTO (the PLUTO points are taken from ref. [1]). Dashed lines $C_l = const$ are drawn through the DELPHI points.

Fig.5 Charged particle multiplicity distributions in the KNO-variables $\psi(z) = < n_{ch} > P(n_{ch})$ versus $z = n_{ch} / < n_{ch} >$ for a) full phase space and b) single hemisphere measured by DELPHI in comparison with TASSO[1] and HRS[7] data.

Fig.6 Energy dependence of the NB parameter k^{-1} resulting from fits to charged multiplicity distributions in full phase space for e^+e^- and μ^+p[34] collisions. The e^+e^- data at lower energies are taken from refs. [1],[7]. The straight lines are fits to the form $k^{-1} = a + b \cdot ln(\sqrt{s}/Q_0)$ ($k^{-1} = a + b \cdot ln(W/Q_0)$) with the best values of b as indicated.

Fig.7 Forward-backward charged particle multiplicity correlations, $< n_F >$ versus n_B, measured by DELPHI a) in the full phase space (open dots) and b) in the central $|y| < 1$ region (full dots) together with straight line fits and the Lund PS (JETSET 6.3) model predictions (stars).

Fig.8 Forward-backward charged particle multiplicity correlations measured by DELPHI for a) unlike sign and b) like sign charged particles in the full phase space (open dots) together with straight line fits and the Lund PS (JETSET 6.3) model predictions (stars).

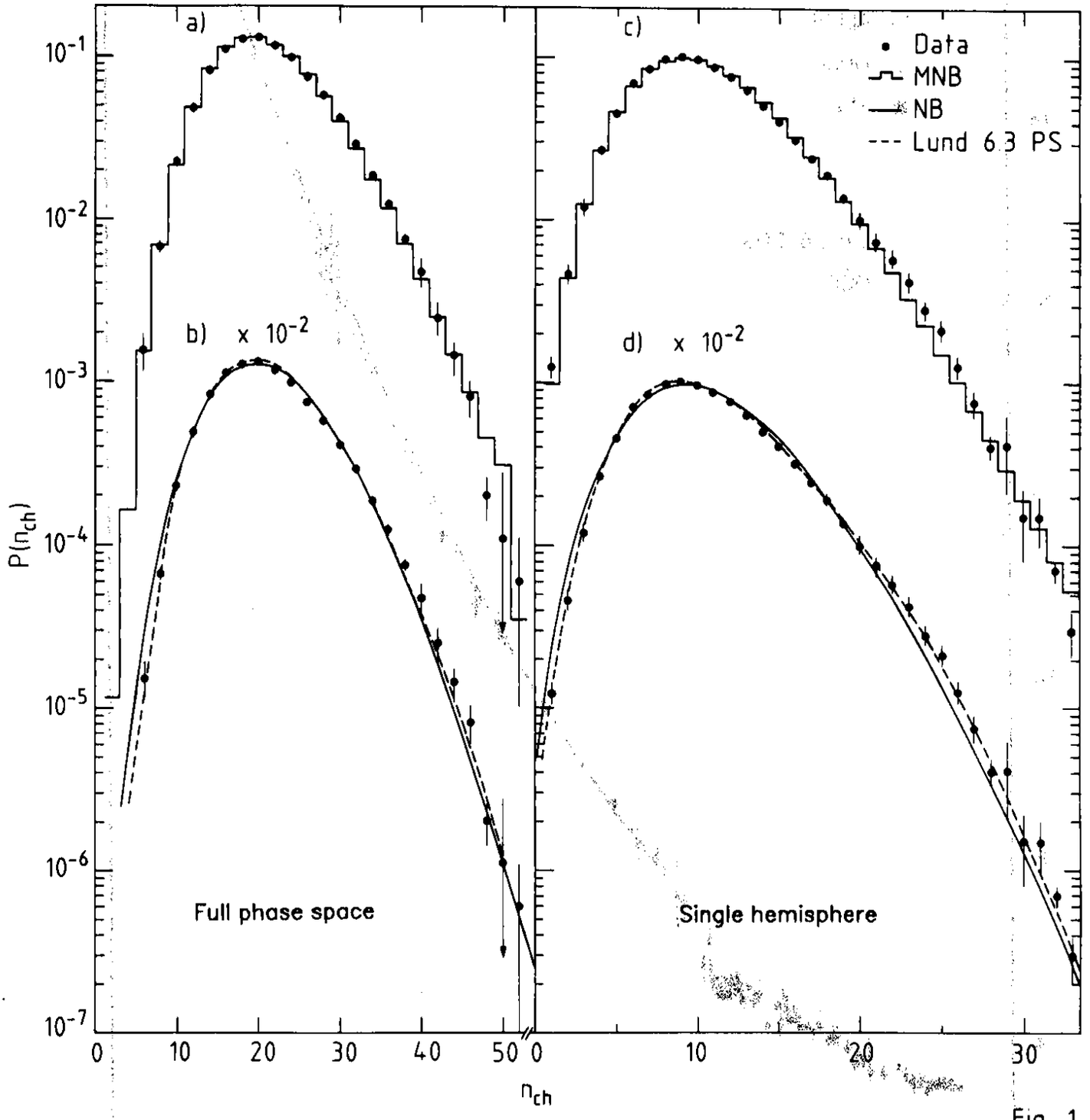
a)
b) x 10^{-2}
c)
d) x 10^{-2}
Data
MNB
NB
Lund 6.3 PS
Full phase space
Single hemisphere
$P(n_{ch})$
n_{ch}
10^{-1}
10^{-2}
10^{-3}
10^{-4}
10^{-5}
10^{-6}
10^{-7}
0
10
20
30
40
50

Fig. 1

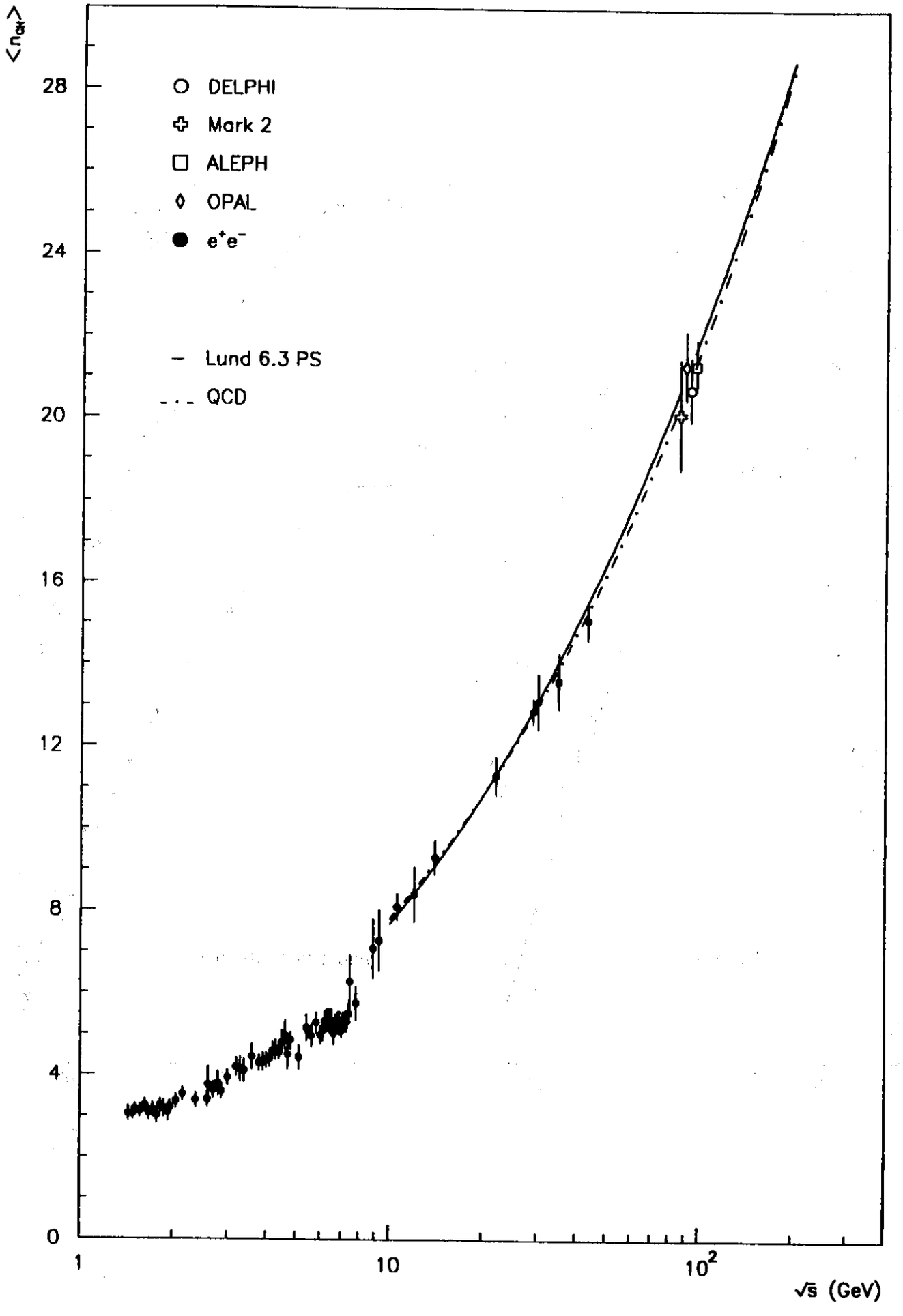
$\langle n_{ch} \rangle$
28
24
20
16
12
8
4
0
1
10
10^2
$\sqrt{s}$ (GeV)
DELPHI
Mark 2
ALEPH
OPAL
e^+e^-
Lund 6.3 PS
QCD

Fig.2

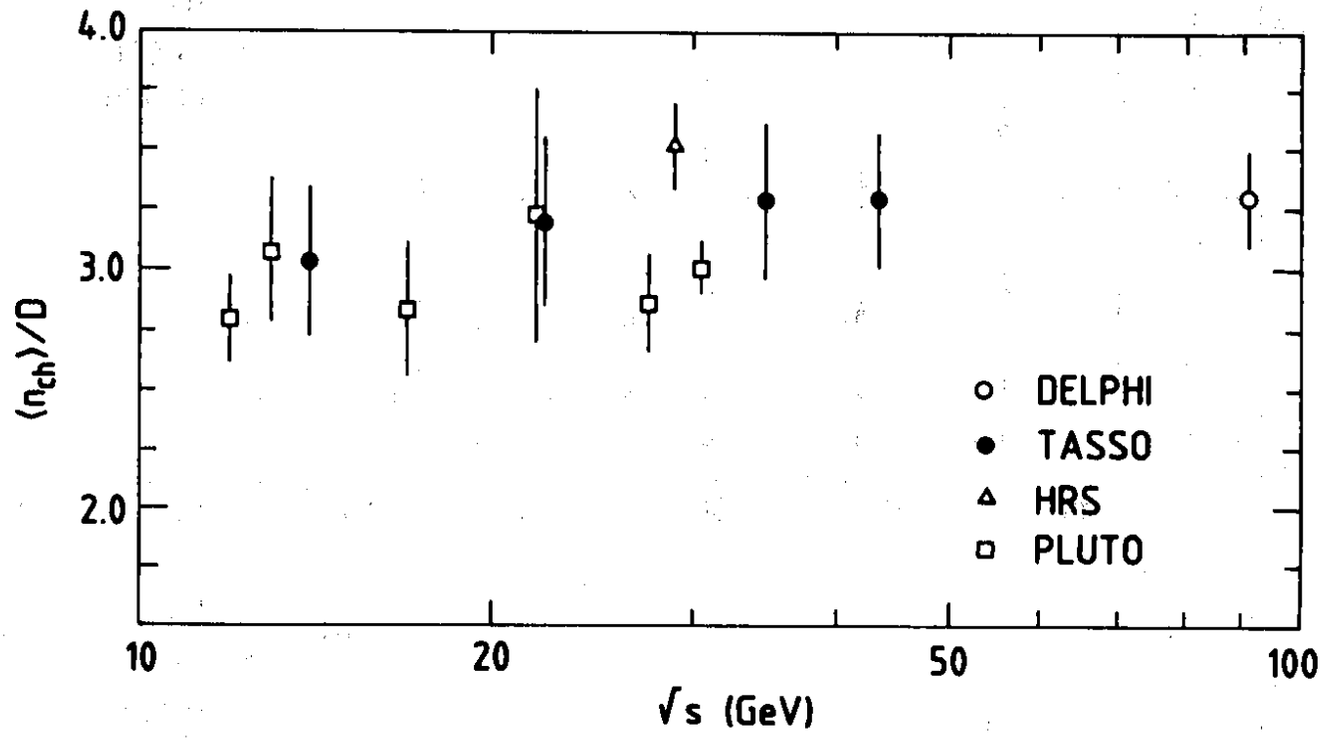

FIG. 3

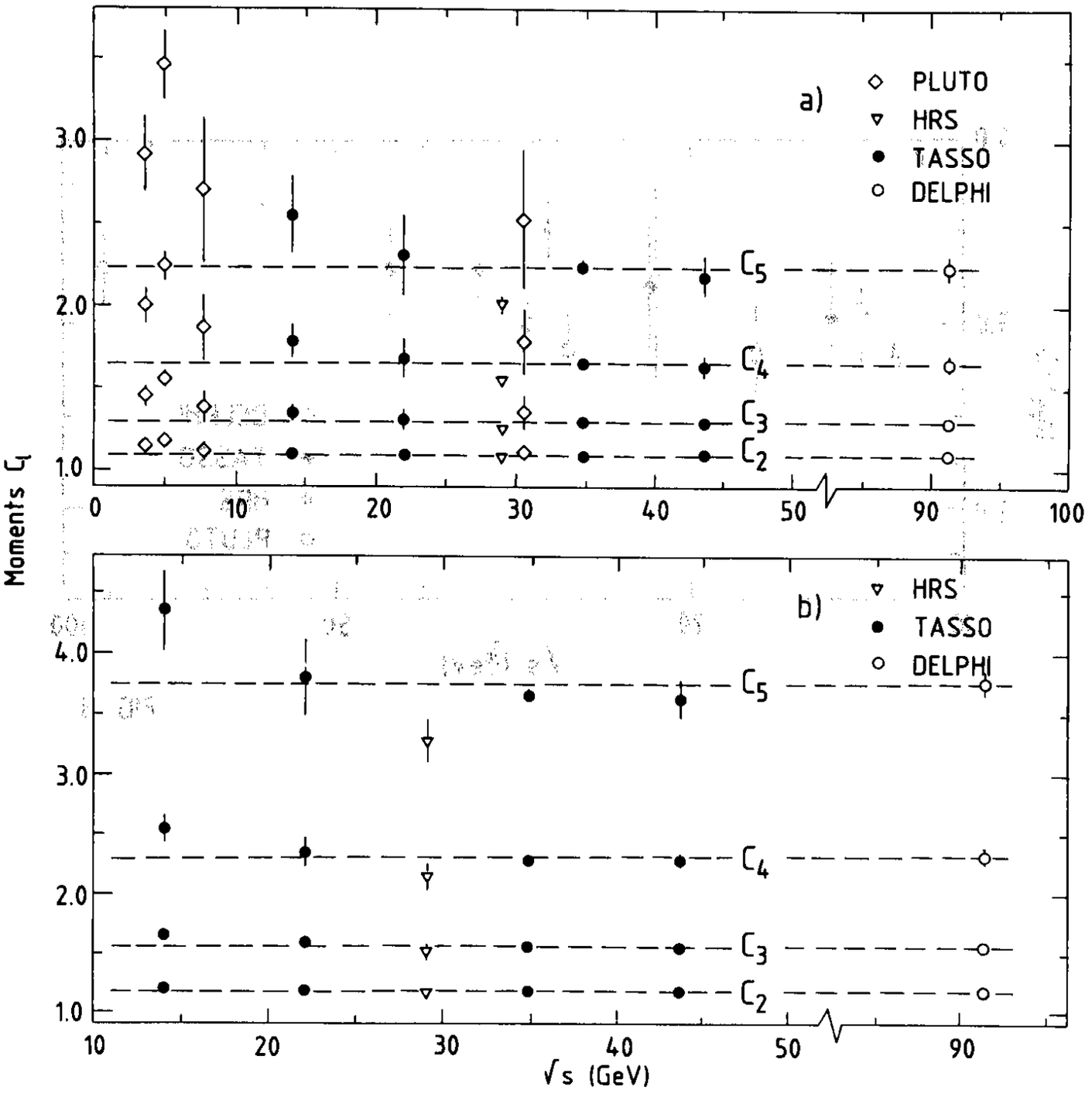
a)
PLUTO
HRS
TASSO
DELPHI
C_5
C_4
C_3
C_2
3.0
2.0
1.0
0
10
20
30
40
50
90
100
b)
HRS
TASSO
DELPHI
C_5
C_4
C_3
C_2
4.0
3.0
2.0
1.0
10
20
30
40
50
90
Moments C_l
$\sqrt{s}$ (GeV)

Fig.4

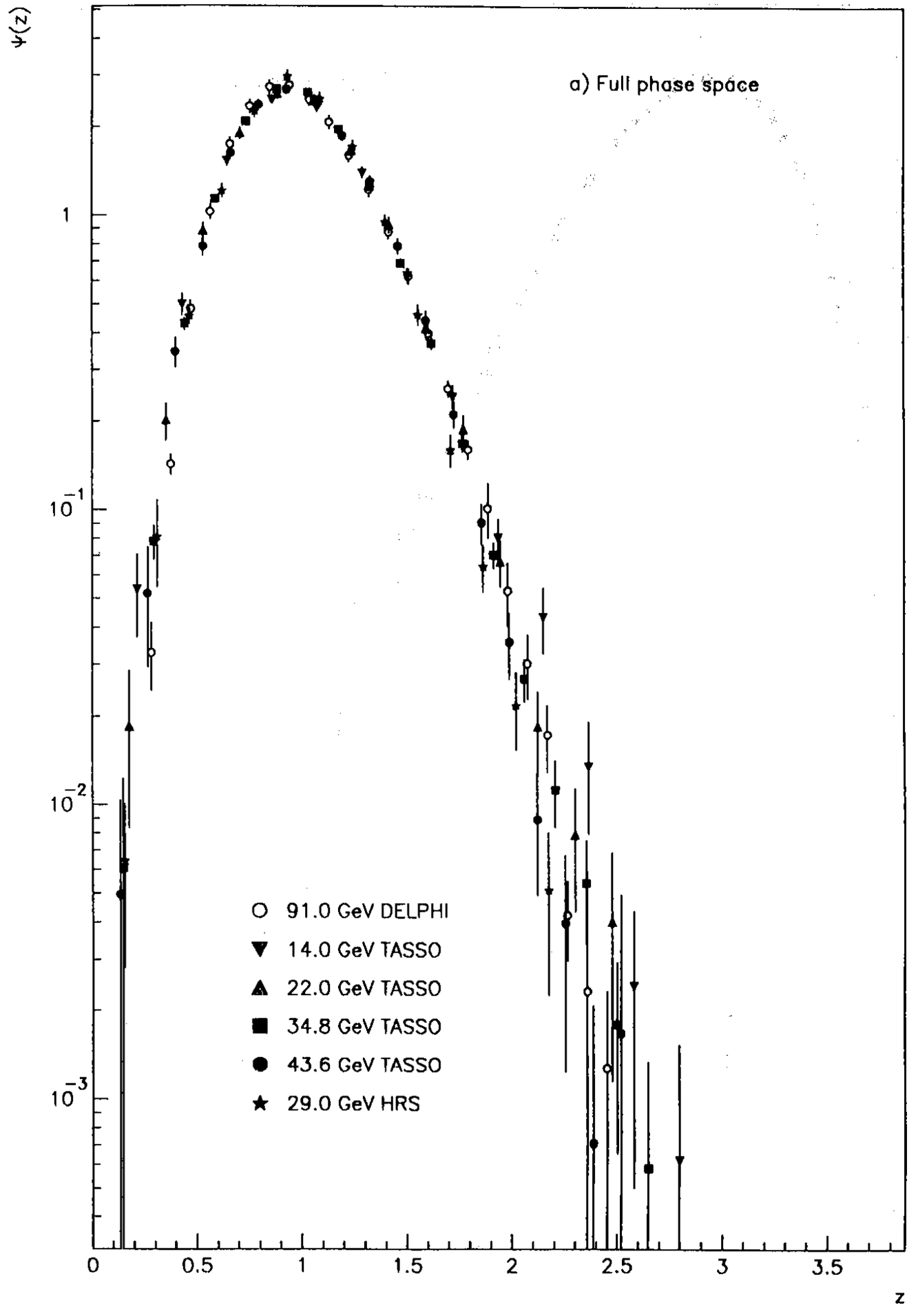
ψ(z)
a) Full phase space
1
10^{-1}
10^{-2}
10^{-3}
0
0.5
1
1.5
2
2.5
3
3.5
z
91.0 GeV DELPHI
14.0 GeV TASSO
22.0 GeV TASSO
34.8 GeV TASSO
43.6 GeV TASSO
29.0 GeV HRS

Fig.5a

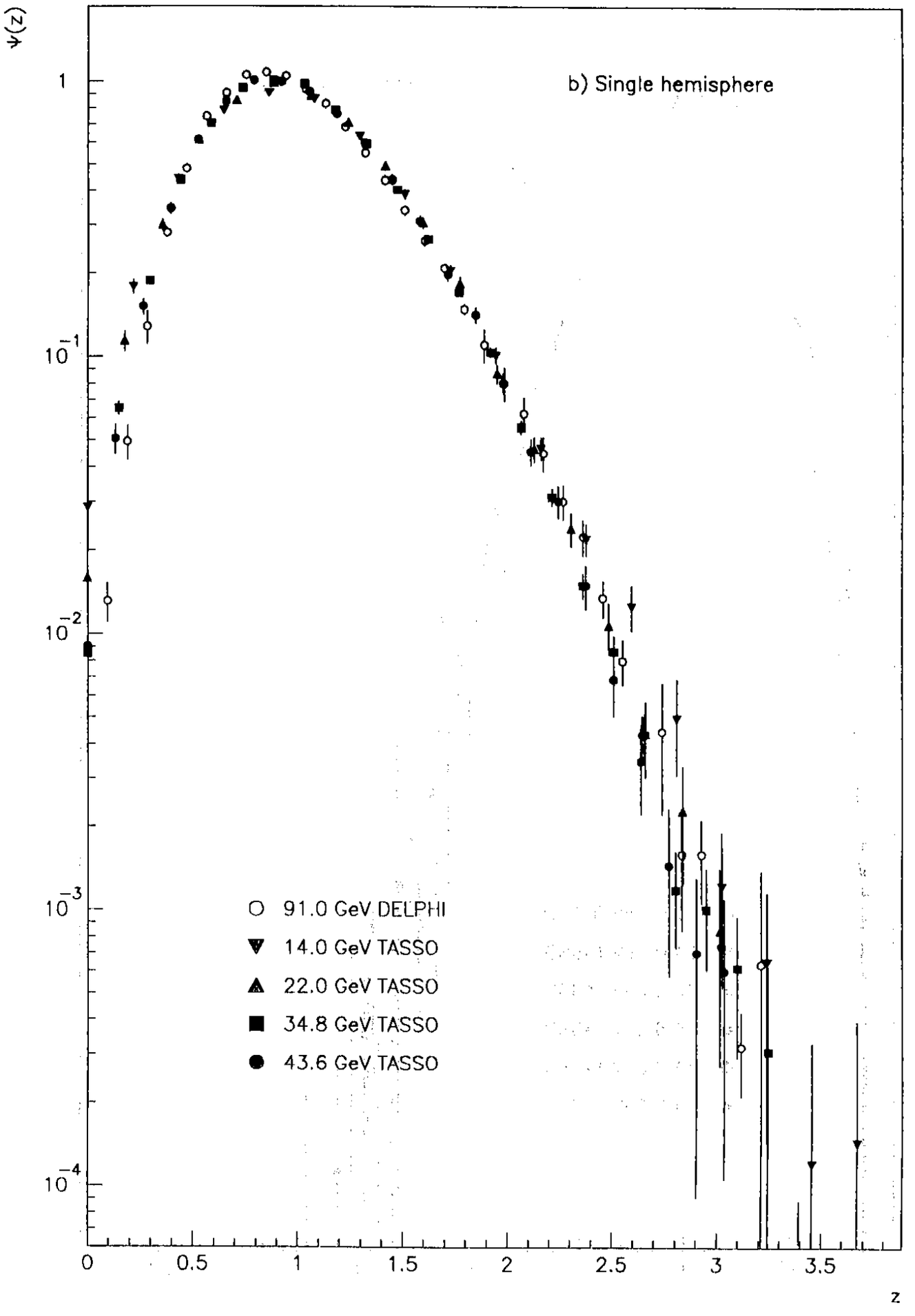
ψ(z)
b) Single hemisphere
1
10^{-1}
10^{-2}
10^{-3}
10^{-4}
91.0 GeV DELPHI
14.0 GeV TASSO
22.0 GeV TASSO
34.8 GeV TASSO
43.6 GeV TASSO
0
0.5
1
1.5
2
2.5
3
3.5
z

Fig.5b

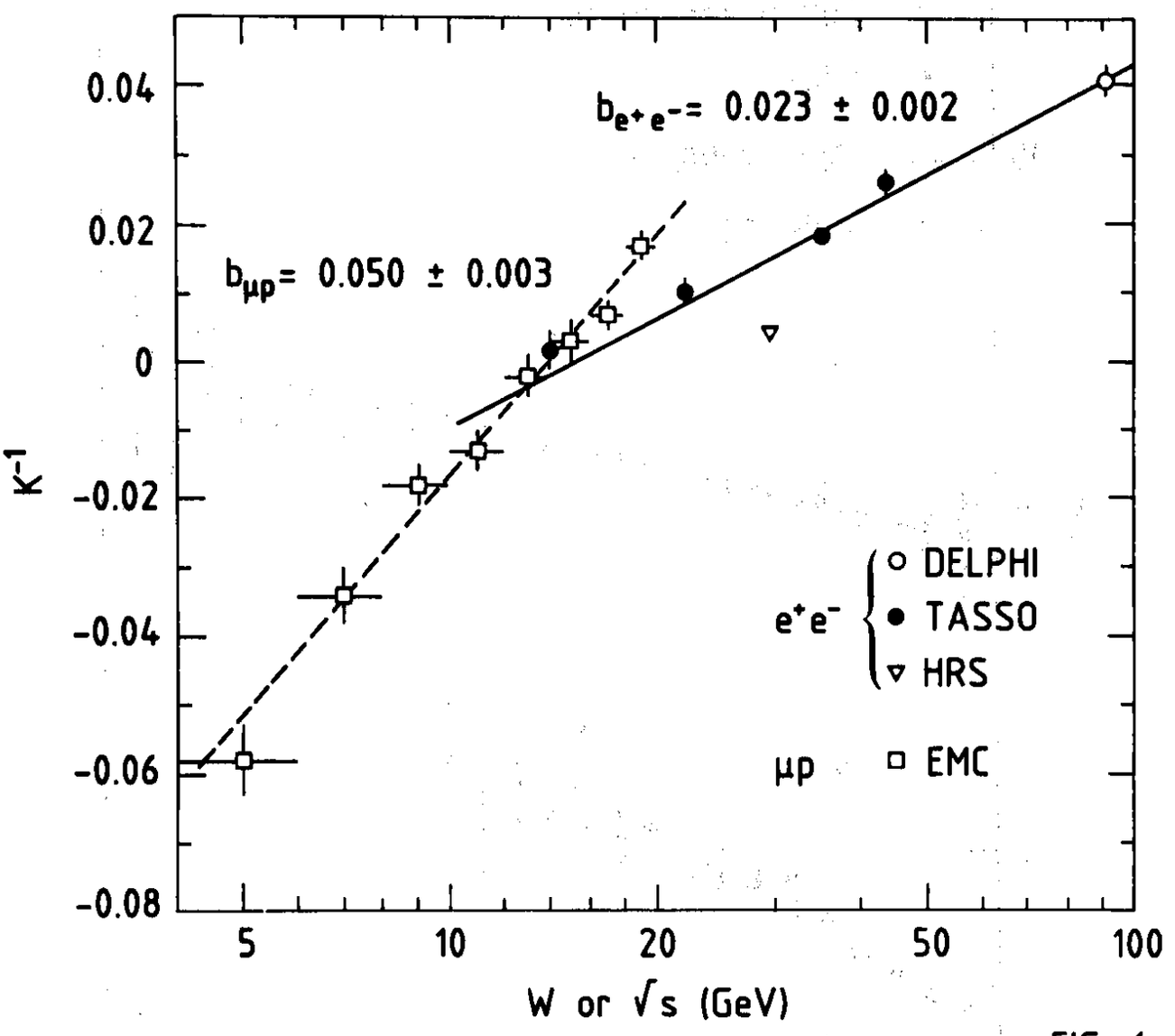
0.04
0.02
0
-0.02
-0.04
-0.06
-0.08
K⁻¹
$b_{e^+e^-}$= 0.023 ± 0.002
$b_{\mu p}$= 0.050 ± 0.003
e⁺e⁻
DELPHI
TASSO
HRS
μp
EMC
5
10
20
50
100
W or √s (GeV)

FIG. 6

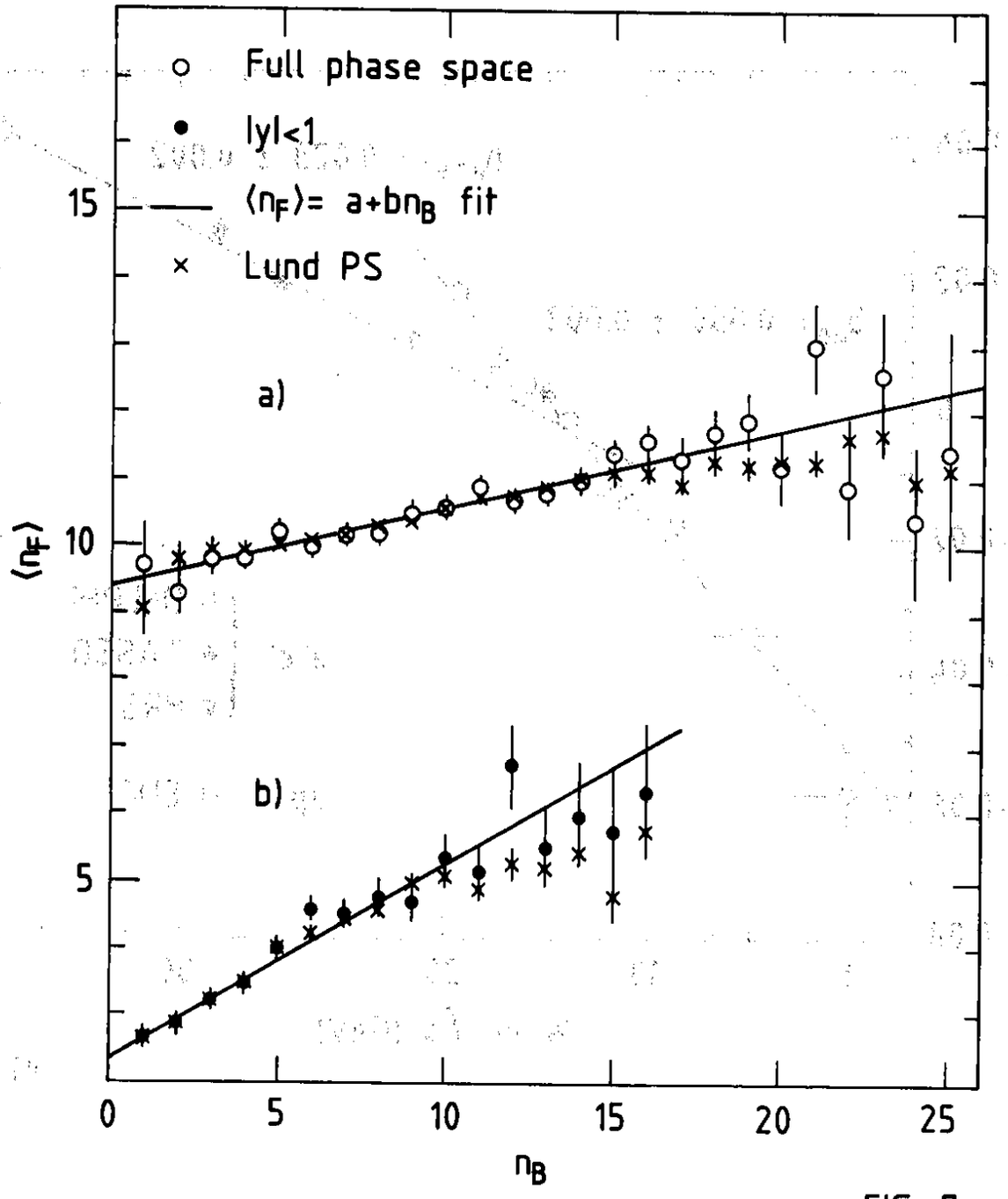

FIG. 7

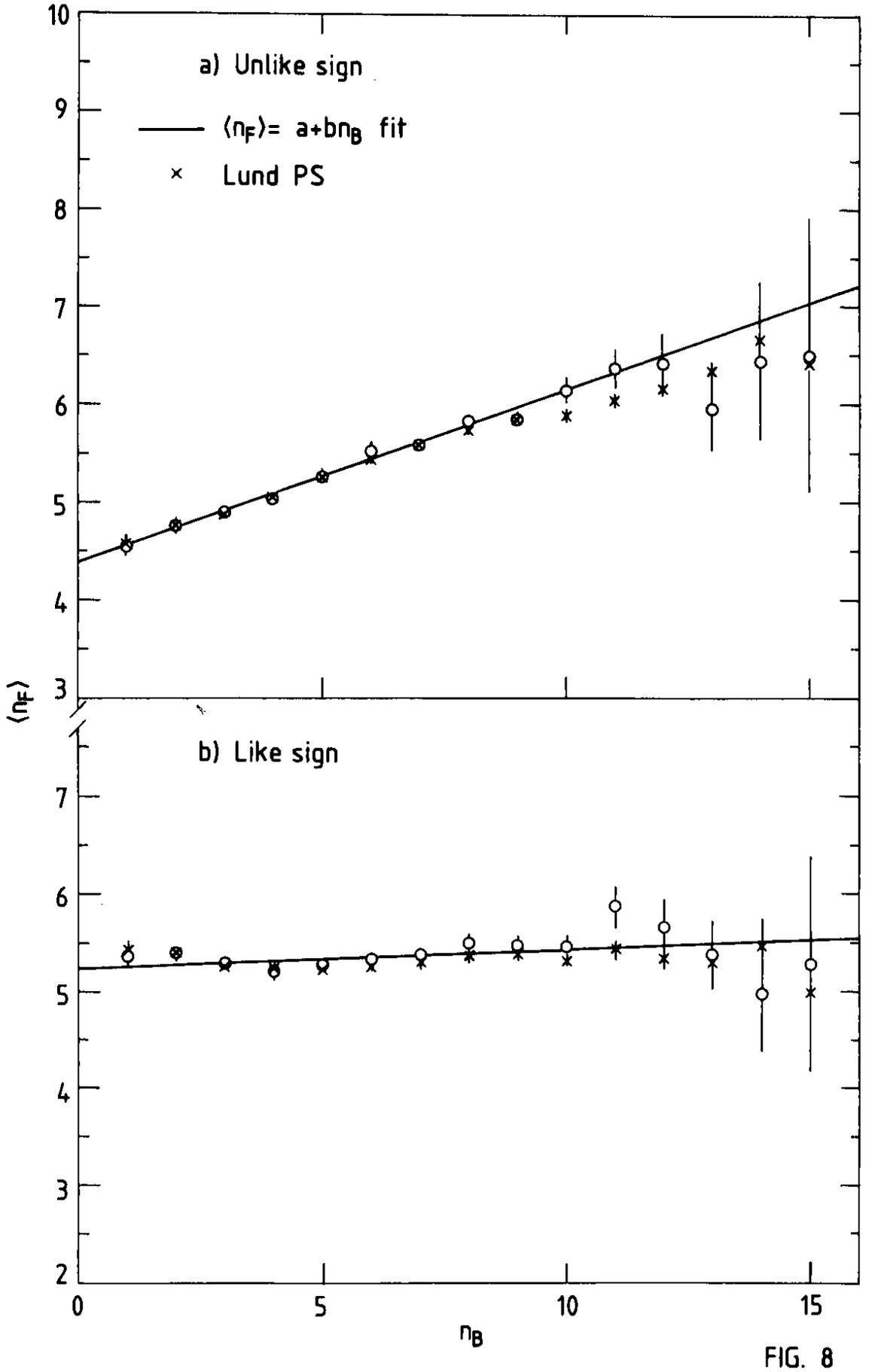

FIG. 8

Imprimé au CERN. Prix : 0.85 Fr.